

## STUDY OF THE SURFACE FINISH AND GEOMETRIC TOLERANCE ATTAINABLE BY SINTER-BASED AM TECHNOLOGIES

Dr. Joseph Tunick Strauss Engineer/President HJE Company, Inc. Queensbury, NY, USA

> Mattia Forgiarini Lead Process Engineer Azoth, Inc Ann Arbor, MI, USA

#### INTRODUCTION

The original impetus for this study was to investigate the use of sinter-based additive manufacturing (AM) to replace or supplement metal injection molding (MIM).<sup>1,2</sup> MIM is a mature powder metallurgy (PM) manufacturing technology that competes well with discrete machining and investment casting. MIM performs best for small parts made in high volumes. Sinter-based AM works well with small parts but with much smaller production volumes. Both MIM and sinter-based AM first produce an intermediate part that is made from metal powder held together with an organic binder. These parts must be debound and sintered. MIM producers have debinding and sintering capacity and would have an advantage to adopting sinter-based AM by leveraging these operations. Thus, if sinter-based AM is able to match the quality of a MIM part but at lower production numbers, its adoption by MIM producers could expand the range of parts offered over a broader production volume scale.

These initial studies reported primarily on parts produced by binder jetting technology (BJT). To provide a more complete comparison of the current sinter-based AM technologies, data was collected from equipment manufacturers and manufacturers using material extrusion (MEX), material jetting technology (MJT), and vat photopolymerization (VPP). This information is compiled and presented so that those considering sinter-based AM can determine if that technology is appropriate with respect to achievable geometric tolerances and surface finishes.

# DESCRIPTIONS OF MIM AND SINTER-BASED METAL AM PROCESSES

All of the sinter-based metal AM technologies and MIM share the following attributes:

- 1. The feedstock is composed of metal powder. The particle size of the powder must be MIM grade (D90 < 30 microns) or finer.
- 2. An organic (polymer) binder is utilized to provide strength and shape to the otherwise loose powder.
- 3. The organic binder must be removed by a debinding operation, which may contain a solvent treatment but always includes a thermal treatment to volatize or "burn off" the binder.
- 4. After debinding, the part is subsequently heated in a controlled atmosphere furnace at elevated temperatures. This process is called "sintering" and results in metallurgical bonding and densification of the powder part.

A brief description of MIM is included for reference.

**Metal Injection Molding**: MIM is a combination of plastic injection molding and powder metallurgy. A MIM feedstock is prepared by combining metal powder and a mixture of polymers. This feedstock is processed by injection molding (heating and injection into a rigid mold) and produces a composite powder/binder part. The part is then debound and subsequently sintered. The need for specific (and expensive) tooling makes this cost-effective for high volumes of parts. There are several instances where MIM is being successfully used to make precious metal jewelry items in production.<sup>3</sup>

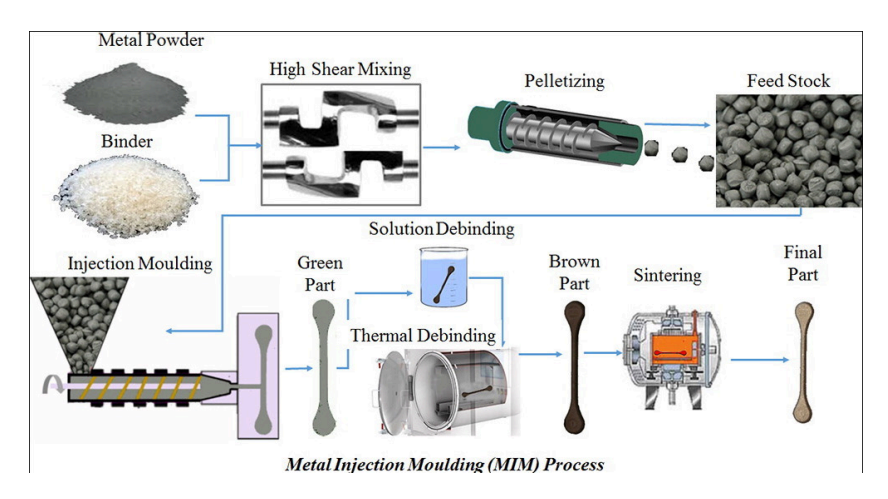


Figure 1: Metal Injection Molding (MIM) process schematic4

**Binder Jetting Technology**: BJT is a powder bed technology. Layers of powder are spread and a liquid binder is deposited onto the powder bed by a print head moving horizontally along the x and y axes of the machine. The binder bonds the powder together. The component is built up layer by layer through the binding action of the liquid, shown in Figure 2.<sup>5</sup> In most cases, the entire build chamber is heated to cure the binder, which usually contains a thermoset epoxy (UV curable epoxy). The printed parts are then debound and sintered to densify the powder into a solid dense metal part. In most cases, support structures are not necessary as the powder bed supports the part during the build and cure.

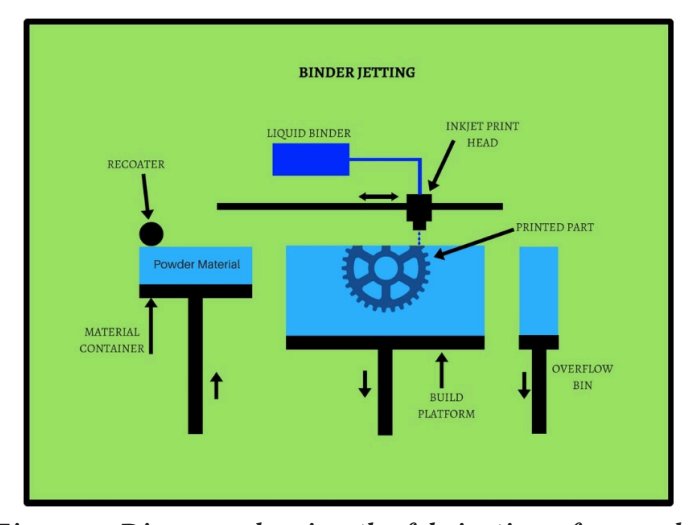


Figure 2: Diagram showing the fabrication of a gear by binder jetting (BJT)<sup>5</sup>

**Material Extrusion Technology**: In MEX, the build material is a metal-filled polymer very similar to MIM feedstock. The build material is heated and extruded through a small nozzle and deposited layer by layer as shown in Figure 3.<sup>6</sup> The print head is also guided by a typical X-Y gantry system. Support material may be the build material or a separate material (usually a ceramic) deposited by a second print head in the gantry. The debinding step may involve a solvent treatment to dissolve one component of the binder. The remaining binder is removed thermally. The debound parts are subsequently sintered.

**Vat Photopolymerization**: In VPP, a thin layer of a slurry, consisting of a photo-curable liquid resin and metal powder, is exposed to a rastered UV laser or a projected light pattern (DLP)

as shown in Figure 4.7 The exposed resin cross-links capturing the metal powder within. The printed parts are subsequently debound and sintered. In some configurations, the resin contains a wax component to facilitate debinding.

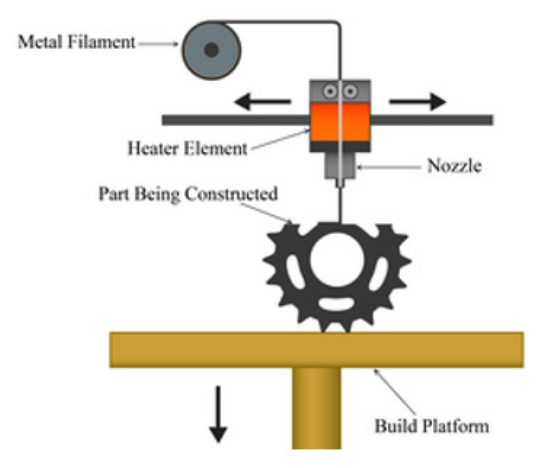


Figure 3: Diagram showing the fabrication of a gear by material extrusion (MEX)<sup>6</sup>

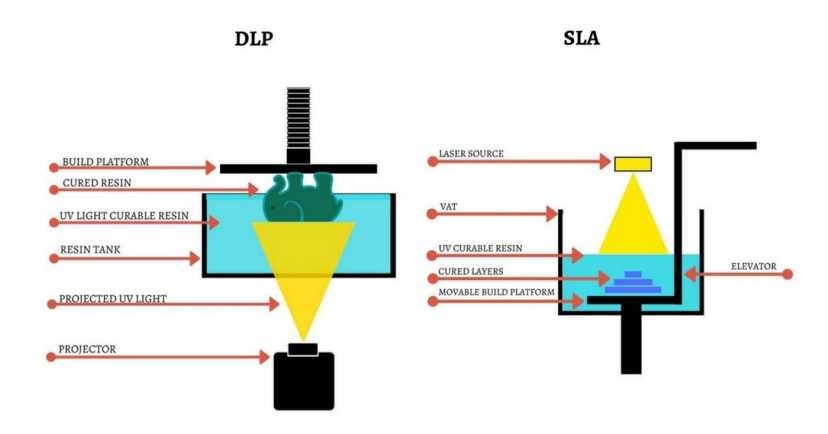


Figure 4: Vat photopolymerization (VPP) showing the DLP configuration (left) and the scanning UV laser configuration (right)<sup>7</sup>

**Material Jetting Technology**: MJT is similar to BJT but does not use a powder bed. Instead, the build material (metal powder) is deposited as a slurry through an inkjet head. The slurry contains components that allow some portion to immediately volatilize and

other components to solidify (cure) to maintain the shape. Since the metal powder is being injected through an inkjet head the particle size must be smaller in size than the MIM-grade powders used in other sinter-based AM. In general, the maximum powder diameter must be below 5 microns. A schematic of MJT is shown in Figure 5.

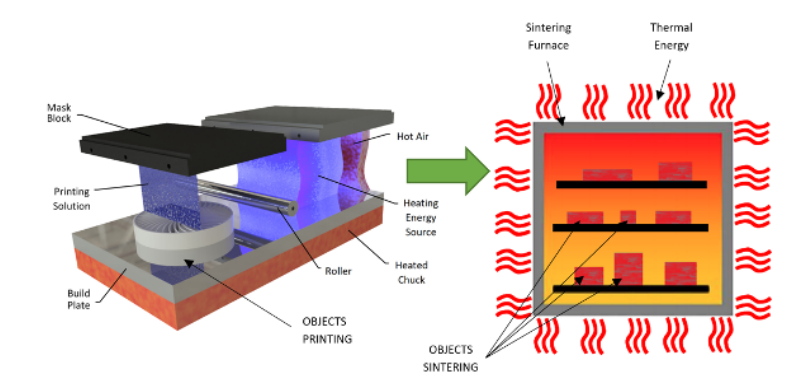


Figure 5: Schematic of metal material jetting (MJT) AM process consisting of 3D printing at room temperature followed by sintering<sup>17</sup>

# SIMILARITIES AND DIFFERENCES BETWEEN MIM AND SINTER-BASED METAL AM

Table 1 summarizes the major process differences between sinter-based AM and MIM. The primary difference is in the part fabrication step. Because of their many processing similarities in the debinding and sintering operations, an economic argument can be made for MIM companies to offer sinter-based metal AM options as the MIM producer should be able to leverage their debinding and sintering operations.

Still, there are differences in the debinding step. Other than MEX, the other sinter-based AM processes entail the use of a UV-curable resin as the binder or a component in the binder formulation. These thermoset polymers are more difficult to remove and/or may leave residual carbon. Thus, changes to the atmospheres used and temperature profiles may be necessary.

Table 1: Process Comparison Between MIM and Non-Fusion Metal AM

Process Step	Similarities	Differences
Powder	These AM technologies need powder with a morphology that allows easy flow or good packing; spherical or near spherical.	
	These AM technologies need small size (typically < 30 µm) to allow densification in sintering without additional force or pressure added.	
		MJT uses powder that is significantly finer than MIM and the other AM methods.
Part Fabrication		MIM needs a tool to be fabricated for the individual part desired, while no tooling is needed for Metal AM.
		While MIM can make complicated geometries, Metal AM has the ability to add additional geometric complexity and internal features that are either difficult or impossible to make with MIM tooling.
		Once MIM tooling is made, part fabrication can be efficient (e.g., one molding cycle can be typically 30 seconds) while in Metal AM the fabrication cycle is typically measured in hours but depending on the part geometry, high numbers can be made in a single pass.
	Both AM and MIM require up- front engineering time and cost, in the case of MIM for tool and process design, for Metal AM development of process parameters and qualification runs.	MIM tooling creates only one part version, while Metal AM (not constrained by hard tooling) can make different part versions for optimal processing.
Debinding	Material extrusion uses the same binders as are used for MIM and thus the same debinding methods can be used.	BJT prints a part with open porosity and a thermoset binder. This enables the part to be debound rapidly using only

	I	a thermal debind. Note: The
		entire build volume is heated
		to a low temperature to cure
		the binder prior to removing
		the parts.
		Some VPP use a one-part
		thermoset binder, which
		requires only a thermal debind.
		Some use a mixture of
		thermoset and thermoplastic
		and require a different
		debinding process.
	AM technologies need high	
Sintering	temperature sintering furnaces to	
	bond and densify the part.	
	AM technologies have a high %	Powder loading for material
	shrinkage (15-25%) from	extrusion using a filament may
	printed part to a sintered	be lower than typical MIM
	densified part.	feedstocks, thus shrinkage will
	(MIM ~10-15% shrinkage.)	be higher.
	AM technologies typically will	
	undergo some amount of	
	distortion/anisotropic shrinkage	
	during sintering.	
		MIM uses conventional setters
		when needed. Material
		Extrusion may have a
		provision to co-print ceramic
		supports. Binder jet and VP
		print technologies may take
		advantage of printing sintering
		supports during the build. This
		has the trade-off of additional
		removal and finishing
		operations but may reduce the
		need for special setters.

## **SUMMARY OF PRIOR STUDIES**

Prior studies<sup>1,2</sup> investigated the potential of using sinter-based metal AM to supplement or even replace MIM. Part cost, attainable tolerance, and surface finish were the primary figures of merit used. The methodology was to pick several MIM parts that represented various levels of difficulty for MIM and have them quoted and produced by the various AM technologies.

 Part cost: With respect to part cost, as expected, the AM technologies could produce parts at a much lower cost than MIM for low production numbers. Conversely, for large production volumes (5,000 and greater), MIM was the lowest cost process. The main cost driver for MIM is the tooling,

- which necessitates large production numbers to amortize the tooling cost.
- 2. Material density: The material density was used as an indication of part integrity and as a surrogate for mechanical properties. The densities achievable by the AM technologies were on par with those for MIM. Thus, it was assumed that the mechanical properties were equivalent.
- 3. Geometric tolerances: This is one area where the AM parts were challenged in meeting MIM requirements, except for a few specific cases.
- 4. Surface finish: This attribute is where MIM currently has a strong advantage over the AM processes. The particular parts chosen for this project had much rougher surface finish requirements than typical MIM parts. Nonetheless, the AM processes, for the most part, were not capable of meeting those requirements, even after aggressive media blasting.

### **Details on the studies**

Three of the manufacturers participating in the studies produced parts for these studies. All three printed parts via BJT. Parts made by MEX, MJT, and VPP were not represented. The BJT parts that were received had been aggressively media-blasted after the sintering operation.

#### **Geometric tolerances**

The tolerance figure of merit chosen in this study is the percentage (percentage = 100\*inch-tolerance/inch-base dimension). This is a general term that describes the ability for a process to meet the goal dimension by normalizing the capability over the size of the part. Generally, to report the process capabilities in this manner, a significant amount of process history is needed. This is not typically found in the research literature. Manufacturers can usually provide this information, and it is reported if made available.

Three parts previously in production by MIM were chosen for the comparison. The three parts represented levels of difficulty for MIM from "easy" to "very challenging" based on specific base measurements, relative locations, and hole/surface radii and diameters. The entities had tolerances between +/- 0.3% and +/- 1.6%. The process capability of MIM is generally considered to be +/- 0.5%, so secondary processes such as coining may be needed to achieve these closer tolerances. From the data collected, the ability for the AM parts to meet the print tolerances appeared to be more a function of the specific manufacturer than the entity tolerance. Only one manufacturer was able to meet all of the

chosen tolerances on one part (inner hook). And one manufacturer essentially missed all of the tolerances on all of the parts.

However, it was recognized that the AM companies had not optimized their process. They only provided the initial parts that were printed. Given the relative ease of modifying the printing parameters (offsets, scaling, etc.) to correct for the final geometry and reiterating a run, it was understood that parts meeting the required tolerances could be achieved in a short time and at a low cost. MIM, on the other hand, may require tooling modifications that are capital- and time-intensive to optimize the process. Thus, it was expected that all of the AM processes could meet the geometric tolerance requirement after optimization from printing modifications and process iterations.

## **Surface roughness**

Two of the parts chosen for these studies are shown in Figure 6. The magazine catch is a gun part and the inner hinge is a medical tool part, both common applications for MIM as they are both produced in large production volumes. The overall lengths of the magazine catch and the inner hinge are approximately 1 in. and 2.2 in., respectively.

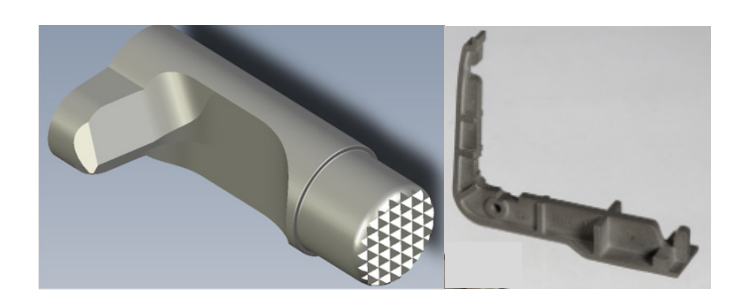


Figure 6: CAD renderings of magazine catch (left) and inner hinge (right)

It has been established that the surface roughness of AM parts is very dependent on the build direction. In general, the surface finish in the plane of the build (X-Y) represents the best surface finish while the surface perpendicular to this plane (Z) or other angles have the highest values for surface roughness. A representative set of the surface roughness was chosen on the inner hook as shown in Figure 7. These areas should represent the best and worst surfaces that these processes can produce, with

respect to a flat plane. The measured surface roughness data is summarized in Table 2. The surface roughness values support the premise that in-plane surface roughness will be better (lower Ra values) than out-of-plane surface roughness.

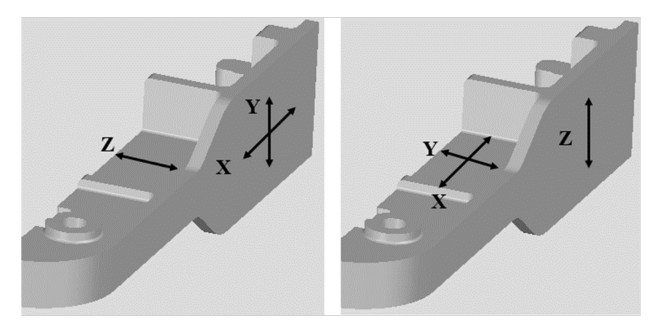


Figure 7: Build orientations for Manufacturer 1 (left) and Manufacturers 2 and 3 (right)

Manufacturer	Print Direction		
	X	Y	Z
1	69	84	100
2	102	98	105

122

3

147

322

Table 2: Summary of surface roughness data, Ra data in μ-inches

In comparison to a "typical" MIM part, Table 3 summarizes some recent surface roughness measurements on a MIM part that was similar to the inner hook.<sup>4</sup> It should be noted that the surface roughness of a MIM part is generally considered isotropic.

Table 3: Summary of surface roughness vs. condition for a flat surface on a typical MIM part;<sup>10</sup> data are an average of 15 measurements on the part

Condition	Ra (μ-in)
As-sintered	23.4
+ Bead blasting	24.2
+ Media tumbling	17.5

In contrast, the magazine catch contained curved surfaces which were, overall, far rougher than the inner hook (Figure 8). The surface roughness measurements across the curved surface exceeded 500 Ra with the part on the left having a slightly lower Ra value than the part in the center. This is a result of the build layer height for the part on the left being smaller than that for the part in the center.

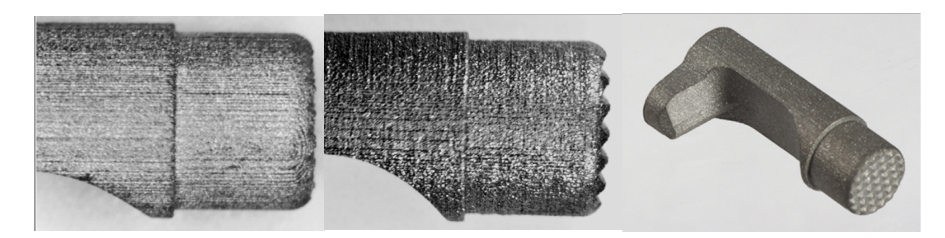


Figure 8: Photographs of the surfaces of two magazine catches; the left part shows a thinner print height than the center part; picture on right for reference

## TOLERANCES AND SURFACE FINISHES OF OTHER SINTER-BASED METAL AM METHODS

The original studies were limited to BJT as the companies representing MEX, MJT, and VPP did not participate in producing actual parts for examination. In order to complete the comparison for this report, other reliable sources were sought. Data was compiled from parts manufacturers, researchers, and equipment manufacturers, both directly and through a literature search.

With respect to geometric tolerances, much of the data reported in the literature references machine resolution or repeatability on shrinkage from sintering, neither of which is a good representation of overall process control. The data presented here is only from sources that specifically address overall process tolerance capability.

Surface roughness data provided in Ra ( $\mu$ -meter) was converted and rounded and is reported here in Ra ( $\mu$ -in) to be consistent.

It must be noted that these other sources represent a wider range of processing including AM equipment and process parameters including materials, powder size, build layer thickness and other build strategies, sintered densities, and measurement techniques. Thus, the reported data embodies a range of values that is representative of the AM process capabilities overall.

Following this section the results and data references will be a summarized in Table 4.

#### **MIM**

As shown in Table 3, the surface finish of MIM is typically in the 20's  $\mu$ -in Ra in the as-sintered conditions. Dry media blasting can actually increase the surface roughness while reductions in surface roughness can be achieved via media tumbling.

MIM process tolerances of +/-0.3% to +/-0.5% and surface finishes of 8-32  $\mu$ -in Ra are commonly reported throughout the MIM industry. Micro-MIM claims to be able to produce surface roughness values as low as 8  $\mu$ -in Ra, using 2-micron powder. Additionally, the sinter shrinkage of MIM is generally considered to be isotropic. While this is not a direct indication of tolerance capability, it does imply a level of consistency and repeatability above that of most AM technologies, which tend to exhibit non-isotropic shrinkage.

#### **BJT**

Munsch et al<sup>14</sup> reported surface finishes for laser powder bed fusion (PBF), MIM, BJT, and MEX. Their data for BJT (XY of 164  $\mu$ -in Ra and Z of 308  $\mu$ -in Ra) is in agreement with that of the part built by Manufacturer #3.<sup>1,2</sup> A comprehensive study of build parameters vs. surface roughness was conducted by Meyers et al.<sup>15</sup> The best surface roughness achieved with an optimized set of build parameters was 162  $\mu$ -in Ra, and the highest value (Z direction on an angled surface) was 391  $\mu$ -in Ra; again, in reasonable agreement with Strauss<sup>1,2</sup> and Schmidt.<sup>14</sup>

A manufacturer practicing both BJT and MJT<sup>16</sup> confirms the findings of the two initial studies for BJT with respect to surface finish capabilities. They are in general agreement with respect to the achievable tolerances of BJT; they claim their process capability to be within +/- 1.5% for new builds which can be reduced to +/- 0.75% on well-designed parts after part-specific optimization.<sup>17</sup>

Another manufacturer using BJT¹8 reports a process tolerance capability of +/- 1.0% with surface roughness in the 150 Ra  $\mu\text{-inch}$  range; again, consistent with others including our base line study.¹-2,16

A study on the optimization of printing parameters to minimize the surface roughness<sup>19</sup> concludes that the build layer thickness is the primary contributor to the surface roughness, especially in the Z direction.

#### **MJT**

There is a very limited amount of production data for metal MJT as there are very few (possibly only one, at the time of this report) used in production in the US. It was shown¹7 that MJT is able to achieve surface finishes for 316 SS of less than 40  $\mu$ -in Ra in the X and Y direction and less than 120  $\mu$ -in Ra in the Z direction for a flat plane. Tolerances realized for MJT are +/- 0.75% on any given entity with a best of +/- 0.5% on well-designed parts after part-specific optimization.

#### **MEX**

The studies on MEX encompassed the widest range for surface finish and tolerance in comparison to the other metal sinterbased AM reported. At least part of this is because MEX is the most widely used AM technology, which is in part due to the low cost of equipment from numerous companies and the availability of a wide range of build materials for both the consumer and industrial markets. Unlike BJT, MJT, and VPP, where there are limited manufacturers of equipment and feedstock, the studies for MEX involved a myriad of machines, which cover a wide range of capabilities. In addition, the studies reflected numerous materials, feedstock forms (filament, rod, and pellet), and process strategies.

Ampower<sup>14</sup> reports on the surface finish data of MEX with a roughness in the XY plane of 216 μ-in Ra and Z of 740 μ-in Ra. Galati and Minetola, 20 printing 17-4 PH, report the lowest surface roughness values found in this study of 60 and 124 u-in Ra for the XY plane and Z planes, respectively for small cubes and 380 and 364 u-in Ra for the XY plane and Z planes, respectively for large cubes. This difference reflects the build layer thickness; the small cubes used a layer thickness of 0.05 mm and the large cubes were printed with a 0.125 mm layer thickness. Small cubes had a process tolerance of +/- 1.8% while large cubes had process tolerances of +/- 2.2%. Incidentally, Akessa et al21 reports that the particle size of the powder used in this feedstock is substantially under 10 microns. Singh et al.<sup>22</sup> used granulated 17-4 PH feedstock in a pneumatic extruder and achieved values of 108 and 144 u-in Ra. The particle size of the feedstock is reported to be between 2 and 10 microns.

Lavecchia et al.<sup>23</sup> compared two different 17-4 PH feedstocks, one made with a wax-polymer (WP) MIM-type formulation and one using a polyoxymethylene (POM) formulation that requires a catalytic debind process. Their surface measurements used a truncated scan (0.8 mm) which limits the true effect of the deposition size and direction. For the WP feedstock they reported

(averaged) 60, 162, and 370 µ-in Ra for the X, Y, and Z axes, respectively. For the POM feedstock they reported (averaged) 156, 240, and 360 μ-in Ra for the X, Y, and Z axes, respectively. This implied that better surface finishes are achieved with the WA feedstock. However, the two materials were printed on different printers with different print strategies. In addition, the layer thickness used may not have been the same and it is not known if the powder particle size in the two build filaments were equivalent. In comparison, Kedziora et al.<sup>24</sup> compared the same 17-4 PH WA feedstock and a 316 SS POM formulation. Again, two different printers were used. It should be noted that the parameters for the conventional-type feedstock were most likely the same between the two studies as they are dictated by the printer. In contrast, they report 326 and 662 u-in Ra for the X and Z axes, respectively. which is significantly different than Lavecchia et al. 23 For the 316 material they report 294 and 300 µ-in Ra for the X, and Z axes, respectively. These studies used different build layer thicknesses (0.125 mm for the 17-4 PH with the WP and 0.150 mm for the 316 SS with the POM binder).

Boschetto et al.  $^{25}$  used the same 316 SS POM feedstock and studied the surface roughness as a function of several build parameters including build layer thickness, extrusion temperature, and deposition speed. The lowest value measured was 96  $\mu$ -in Ra with other, less-optimized builds having surface roughness values as high as 448  $\mu$ -in Ra. This shows that the build parameters can have a significant influence on the surface roughness, outside of the layer thickness and the directional (XY vs Z) effects.

Kluczynski et al.<sup>26</sup> and O'Connor et al.<sup>27</sup> used the same material (POM 316SS) and the same manufacture of printer. They reported surface roughness values of 156 to 224  $\mu$ -in Ra.<sup>27</sup> However, their build strategies differed significantly.

Suwanpreecha et al.  $^{28}$  printed 17-4 parts using a different system and feedstock. The particle size of the powder in this feedstock was much coarser (D50 greater than 10 microns) than the other 17-4 PH feedstocks reported in this paper. Using a layer thickness of 0.15 mm, they achieved surface roughness values of 264 and 632  $\mu$ -in Ra for the X and Z axes, respectively.

It is to be noted that these studies are not direct comparisons but the data is still valid as it indicates the wide range of various process capabilities across the MEX space.

#### **VPP**

VPP systems for processing polymers are well represented in AM manufacturing with numerous manufacturers of equipment and a myriad of polymer systems. However, there are only a few equipment manufacturers that have specifically integrated metal powder into the build capabilities.

Harakaly et al.<sup>29</sup> used MIM-grade powder loaded to 55% solids in their VPP slurry, making it similar to MIM feedstock. The powders had D90's of 22, 16, and 10 microns. Reducing the powder size from a D90 of 22 microns to a D90 of 16 microns reduced the surface roughness from 79 to 59  $\mu$ -in Ra for 316L powder, and from 79 to 60  $\mu$ -in Ra for 17-4 PH powder. However, further reductions in particle size did not reduce the surface finish values. This is attributed to a non-optimized process. It was also noted that the ability to produce fine (smaller) feature resolution was enhanced with the use of finer powders.

Burkhardt et al.³° reported on 316 SS with surface roughness value of 50  $\mu$ -in Ra and a process tolerance capability of +/-0.5%. The tolerance capability is in agreement with VPP for an overall value but adds that for most builds the tolerance range is typically +/0.3 to +/-0.4% with this value increasing above +/-0.5% when referenced to intra-part features around 100 microns.

Melentiev et al.<sup>31</sup> made VPP prints with a 0.025 mm layer thickness. The surface roughness data reported is in close agreement with Harakaly et al.<sup>29</sup> and it is also reported that the sintering shrinkage is nearly isotropic as opposed to other metal sinter-based AM processes.

Harkaly et al.<sup>32</sup> reports 316 SS parts sintered with a surface roughness of 94  $\mu$ -in Ra were able to be polished to a surface roughness less than 3  $\mu$ -in Ra with only 80 microns of material removed from the surface.

Burkhardt $^{33}$  reports surface roughness values up to 240  $\mu$ -in Ra and mentions that the shrinkage is isotropic.

Work done in conjunction with Strauss<sup>1,2,34</sup> measured two VPP parts printed from 316 SS. Figure 9 shows the surface roughness values for the parts in various orientations. The values measured are in good agreement with the other VPP data summarized above.



Figure 9: VPP printed parts with surface roughness in  $\mu$ -in Ra

#### **DISCUSSION**

Table 5 is a summary of the data presented in Table 4 for a more concise view. The data collected encompasses a very wide range of surface finishes and tolerances. One cannot definitively choose which process is optimum for a particular part or application. With respect to jewelry applications, surface finish is paramount. And, related to this, the amount of material that must be removed to achieve the required surface finish is crucial to the economics of the operation.

It is acknowledged that the Ra measure for surface roughness is not as good an indicator as Rt with respect to how it is related to the amount of material removal needed to achieve the desired finish. However, Ra was the most common measure reported in the majority of the studies and it is still a representative indication of the amount of material removal that is needed.

With respect to surface finish and MIM, it is acknowledged that better surface finishes are achieved using finer powders<sup>35</sup> and higher loading factors in the feedstock.<sup>36</sup> Since the metal sinterbased AM technologies are powder metallurgy technologies by default, and are fundamentally similar to MIM with respect to debinding and sintering being an integral part of the process, the same rules will apply; finer powder and higher material loading in the print feedstock will result in lower surface roughness values.

The studies reviewed in this report covered numerous printing parameters for each technology. Within technologies (primarily MEX), there appear to be some complex relationships between process parameters and surface roughness. However, among the various technologies, it appears that those technologies that can print thinner layers have an advantage in producing finer surface finishes.

Table 4: Summary of sinter-based technologies and capabilities

Method	Ra, μ-in	Tolerance, +/- %	Comments	Ref.
MIM	8-32	0.3 to 0.5	Conventional MIM	11,12
MIM	8	0.3	Micro-MIM, 2 micron powder	13
BJT	69-150	>1	XY	2
	100-312		Z	
	>500		Curved surface	
BJT	164/308		XY/Z	14
BJT	162/391		XY/Z	15
BJT	240	1.5 typ./0.75 opt.		17
BJT	150	1		18
BJT	320 max		Non-isotropic shrinkage	33
MJT	<40	0.75 typ./0.50 opt.	XY plane	17
	<120		Z plane	
MEX	216/740		XY/Z	14
MEX	60/124	1.8	Small cubes, 17-4 PH, 0.05 mm layer thickness	20
	380/364	2.2	Large cubes, 17-4 PH, 0.125 mm layer thickness	
MEX	108 to 144		17-4 PH, fine powder	22
MEX	60/162/370		X/Y/Z conventional binder 17-4 PH	23
	156/240/360		X/Y/Z catalytic binder 17-4 PH	
MEX	326/662		X/Z 17-4 PH conventional binder	24
	294/300		X/Z 316 catalytic binder	
MEX	96		Optimized, 316 catalytic binder	25
	448		Not optimized, 316 catalytic binder	
MEX	156-224		316 catalytic binder	26
MEX	774		316 catalytic binder	27
MEX	264/632		X/Z ,17-4 PH	28
VPP	160			
VPP	79		316 SS D90 22 microns	29
	59		316 SS D90 16 microns	
	79		17-4 PH S D90 22 microns	
	60		17-4 PH S D90 16 microns	
VPP	50	0.5		30
VPP		0.3/0.4	typical	32
		0.5	For small features (100 microns)	
VPP			Layer thickness 0.025 mm	31
			Isotropic shrinkage	
VPP	94		As-sintered	32
	3		Polished 80 microns removed	
VPP	Up to 240		Isotropic shrinkage	33
VPP	38-103		Various parts and directions	34

	_		•
Method	Ra, μ-in	Tolerance, +/- %	Comments
MIM	8-32	0.3 to 0.5	Conventional MIM
MIM	8	0.3	Micro-MIM, 2 μ powder
BJT	100 ->500	1.5, 0.75	Tol. typical/optimized
			Highest Ra on curved
			surface.
MJT	40-120	0.75, 0.5	Tol. typical/optimized
MEX	100 to >700	1.8 to 2.2	Tol. size dependent
V/DD	50 to 150	0.5.03	Tol typical/ontimized

Table 5: Summary of data from Table 4

Other than the surface roughness reported for the part in Figure 7 (magazine catch), all the other collected data were taken from flat planes on the parts. Thus, the reported surface finish data presented here represents the best surface finishes achievable from the various AM technologies. A curved surface will produce higher surface roughness values due to the layering or the staircase effect of layer-wise manufacturing,<sup>37</sup> which is ubiquitous to all AM to one extent or another. Thus, any of these processes will produce rougher surfaces for off-axis or curved surface, which essentially characterizes most jewelry items.

To minimize the negative contribution to surface roughness caused by layering, minimizing the layer thickness is fundamental. However, this is not without its own disadvantages. Thinner layers require finer powder, which will cost more. Printing thinner layers requires more time, which also increases manufacturing costs.

One advantage of using finer powders is that higher sintered densities are more readily achieved.<sup>38</sup> The effect on sintered density and jewelry polished is not well-documented in the literature, however, densities above 95% and special polishing techniques will produce a jewelry-quality finish.<sup>3</sup>

The use of one sinter-based AM process versus another is not a straightforward choice for precious metals. The final cost of the piece is a complex function that includes capital equipment and use cost, powder cost, and finishing cost. The cost differential between precious metal alloys could determine which process is used for which material system. Processes that produce AM parts at a lower cost but require extensive finishing may be more suitable for silver alloys with respect to material loss. In contrast, systems that print thinner layers using finer powders and with lower material loss from finishing may be better suited for gold and platinum alloys.

The data reported was predominantly for stainless steel. Every sinter-based system has been successfully used to produce stainless steel parts either in testing or production. At this time, there are no sinter-based systems specifically designed for use with precious metals. However, if the system has been proven for copper it will also work with silver and gold-based jewelry alloys.<sup>3</sup>

### **CONCLUSIONS**

There are several metal sinter-based AM that have potential to produce jewelry items.

Although the geometric tolerance capabilities of these systems lag behind MIM, they are similar to those of investment casting. However, one of the advantages of AM is that tuning the build to produce parts that are within the required geometric tolerance is simply a scaling issue that can be resolved by reiterative print cycles, a relatively low time and cost intensive undertaking.

Since surface finish is an important manufacturing and design factor in jewelry, AM processes that are capable of printing smaller build layer thicknesses may have an advantage from a post-process finishing cost perspective.

#### **ACKNOWLEDGMENTS**

The authors would like to thank Matt Bulger (ATPM Consulting) and Michael Stucky (Norwood Medical) for their assistance and proffering of needed information and insight.

#### **REFERENCES**

- J. Strauss et al., "Evaluation of AM Technologies in MIM Applications: Part 1," International Conference on Powder Metallurgy & Particulate Materials, June 23-26, 2019, Phoenix, AZ.
- 2. J. Strauss et al., "Evaluation of AM Technologies in MIM Applications: Part 2," International Conference on Powder Metallurgy & Particulate Materials, June 20-23, 2021, Orlando, FL.
- 3. J. Strauss, "Current Developments in Powder Metallurgy-Based Manufacturing Technologies for Precious Metals," The Santa Fe Symposium on Jewelry Manufacturing Technology 2022, ed. Eddie Bell (Albuquerque: Met-Chem Research, 2022): 577-596.

- 4. https://www.sciencedirect.com/science/article/abs/pii/S0032591017305120
- 5. https://manufactur3dmag.com/binder-jetting-works/
- https://news.3deo.co/metal-3d-printing-processes-fdmfff
- 7. https://manufactur3dmag.com/difference-dlp-sla/
- 8. Private communication, Matthew Bulger, ATPM Consulting, Dec. 3, 2024.
- 9. P. Delfs et al., "Surface Roughness Optimized Alignment of Parts for Additive Manufacturing Processes," 2015 International Solid Freeform Fabrication Symposium, August 10-12, Austin, TX.
- 10. Norwood Medical, Dayton, Ohio, internal data.
- 11. BRM, Shanghai, China, online technical brochure: https://www.atmsh.com/en/product/products-1-54. html#mcetoc\_1gk9pq7lt57
- Parmatech Corporation, Petaluma, CA, online technical brochure: https://atwcompanies.com/wp-content/ uploads/2021/07/Power-of-Powder-MIM-Design-Guide. pdf
- Micro MIM Japan, technical newsletter, Vol. 13, Nov. 25, 2019, https://micro-mim.eu/sys/wp-content/uploads/2019/11/MMJ\_013\_EN.pdf
- 14. M. Schmidt, et al., "Binder Jetting and FDM: A Comparison with Laser Powder Bed Fusion and Metal Injection Molding," Metal Additive Manufacturing, Vol. 4, No. 3, 2018 Inovar Communications.
- 15. K. Meyers, et al., "The Effect of Print Speed on Surface Roughness and Density Uniformity of Parts Produced Using Binder Jet 3D Printing," 2019 International Solid Freeform Fabrication Symposium, August 12-14, Austin, TX.
- 16. Azoth, 3D, Ann Arbor, MI.
- 17. M. Forgiarini, C. Cochran, "Metal Binder Jetting and Metal Material Jetting as Complementary Technologies: a User Perspective," Azoth3D white paper: https://www.azoth3d.com/white-paper/
- DSB Technologies, Powder Metallurgy Process Matrix download, https://www.dsbtech.com/powder-metalprocess-downoad?submissionGuid=2cOf5a75-4c66-4a18-a161-31e56cf4beb7

- H. Chen and Y. F. Zhao, "Process Parameters Optimization for Improving Surface Quality and Manufacturing Accuracy of Binder Jetting Additive Manufacturing Process," Rapid Prototyping Journal, 22/3, (2016): 527-538.
- 20. M. Galati and P. Minetola, "Analysis of Density, Roughness, and Accuracy of the Atomic Diffusion Additive Manufacturing (ADAM) Process for Metal Parts," *Materials*, 12, (Dec. 2019): 4122.
- 21. A. Akessa et al., "Investigations of the Microstructure and Mechanical Properties of 17-4 PH SS Printed Using a Markforged Metal X," *Materials*, 152, (Oct. 2022): 6898.
- 22. G. Singh et al., "Additive Manufacturing of 17-4 PH steel using Metal Injection Molding Feedstock: Analysis of 3D extrusion Printing, Debinding and Sintering," Additive Manufacturing, Volume 47, (Sep. 2021): 102287
- 23. F. Lavecchia et al., "Comparative Study on the Properties of 17-4 PH Stainless Steel Parts Made By Metal Fused Filament Fabrication Process and Atomic Diffusion Additive Manufacturing," Rapid Prototyping Journal, 29/2, (Jul. 2022): 393-407.
- 24. S. Kedziora et al., "Strength Properties of 316K and 17-4 PH Stainless Steel Produced with Additive Manufacturing," Materials, 15, (2022): 6278.
- 25. A. Boschetto et al., "Roughness Investigation of Steel 316L Parts Fabricated by Metal Fused Filament Fabrication," *Journal of Manufacturing Processes*, Volume 81, (Jun. 2022): 261-280.
- 26. J. Klucznski et al., "A Comparative Investigation of Properties of Metallic Parts Additively Manufactured Through MEX and PBF-LB/M Technologies," *Materials*, 16, (Jul. 2023): 5200.
- 27. H. O'Connor et al., "Fused Filament Fabrication Using Stainless Steel 316L-Polymer Blend: Analysis and Optimization for Green Density and Surface Roughness," Polymer Composites, 45, (Apr. 2024): 10632-10644.
- 28. C. Suwanpreecha et al., "Effects of Aging and Shot Peening on Surface Quality and Fatigue Properties of material Extrusion Additive Manufactured 17-4PH Stainless Steel," Materials & Design, 241, (Apr. 2024): 112939.
- 29. G. Harakály et al., "Material Selection for Lithography-Based Metal Manufacturing of Components with Intricate Features and High Surface Quality," *International*

- Conference on Powder Metallurgy & Particulate Materials, June 16-19, 2024, Pittsburgh, PA.
- 30. C. Burkhardt et al., "Lithography-Based Metal Manufacturing of Jewelry and Watch Cases Made From 316L Stainless Steel and Titanium Alloys," The Santa Fe Symposium on Jewelry Manufacturing Technology 2022, ed. Eddie Bell (Albuquerque: Met-Chem Research, 2022): 47-60.
- 31. R. Melentiev et al., "High-Resolution Metal #D Printing via Digital Light Processing," Additive Manufacturing, 85, (Apr. 2024): 104156.
- 32. G. Harakály et al., "The Applicability of Lithography-Based Metal Manufacturing for 316L Stainless Steel," Euro PM2023 Proceedings, Oct. 1-4, Lisbon.
- 33. C. Burkhardt, "A Beginner's Guide to Three leading Sinter-Based Metal Additive Manufacturing Technologies," *Powder Injection Molding International*, Vol. 14, No. 1, (Mar. 2020): 69-79.
- 34. HJE Company, Inc., Queensbury, NY internal R&D 2019.
- 35. S. Greiner et al., "Influence of Material and Processing Parameters on the Surface Roughness of Injection-Molded Ceramic Parts," Journal of Ceramic Science and Technology, Vol. 08, No. 2, (2017): 277-286.
- 36. M. von Witzleben and T. Moritz, "Ceramic Injection Molding." Encyclopedia of Materials: Technical Ceramics and Glasses (2021): 179-188.
- 37. D. Ahn et al., "Fabrication Direction Optimization to Minimize Post-Machining in Layered Manufacturing," *Int. J. Mach. Tools Manuf.*, 47, (2007) 593–606.
- 38. F. Lenel, *Powder Metallurgy Principles and Applications*, (Princeton, NJ, Metal Powder Industries Federation, 1980), 218-219.